

Research Article

FDTD Modeling of a Cloak with a Nondiagonal Permittivity Tensor

Naoki Okada and James B. Cole

Graduate School of Systems and Information Engineering, University of Tsukuba, 1-1-1 Tennodai, Tsukuba, Ibaraki 305-8573, Japan

Correspondence should be addressed to Naoki Okada, okada@cavelab.cs.tsukuba.ac.jp

Received 13 February 2012; Accepted 27 March 2012

Academic Editors: A. Danner, M. Midrio, and A. Tervonen

Copyright © 2012 N. Okada and J. B. Cole. This is an open access article distributed under the Creative Commons Attribution License, which permits unrestricted use, distribution, and reproduction in any medium, provided the original work is properly cited.

We demonstrate a finite-difference time-domain (FDTD) modeling of a cloak with a nondiagonal permittivity tensor. Numerical instability due to material anisotropies is avoided by mapping the eigenvalues of the material parameters to a dispersion model. Our approach is implemented for an elliptic-cylindrical cloak in two dimensions. Numerical simulations demonstrated the stable calculation and cloaking performance of the elliptic-cylindrical cloak.

1. Introduction

An optical cloak enables objects to be concealed from electromagnetic detection. Pendry et al. developed a method to design cloaks via coordinate transformations [1]. The coordinate transformation is such that light is guided around the cloak region. Material parameters (permittivity and permeability) can be obtained in the transformed coordinate system and put into Maxwell's equations. This approach enables one to design not only cloaks but also other metamaterials that can manipulate light flow. For example, concentrators [2], rotation coatings [3], polarization controllers [4–6], waveguides [7–11], wave shape conversion [12], object illusions [13–15], and optical black holes [16, 17] have been designed. However, not many metamaterials have been realized in the optical region [18–25], because material parameters given by coordinate transformations have complicated anisotropies.

Numerical simulations are useful to analyze complicated metamaterial structures. In this paper, we present a finite-difference time-domain (FDTD) analysis of a cloak. The FDTD method has gained popularity for several reasons: it is easy to implement, it works in the time domain, and its arbitrary shapes can be calculated [26–29]. FDTD modelings of cloaks with a diagonal (uniaxial) permittivity tensor have been demonstrated [30–38], but a cloak with a nondiagonal permittivity tensor has never been calculated by the FDTD

method. The diagonal case can be stably calculated by mapping material parameters having values less than one to a dispersion model [31]. However, we found that mapping the nondiagonal elements to dispersion models causes the computation to diverge.

In this paper, we analyze the numerical stability for a cloak with a nondiagonal permittivity tensor and derive the FDTD formulation. We apply our method to simulate light propagation in the vicinity of an elliptic-cylindrical cloak. To the best of authors' knowledge, this is the first time that a cloak with a nondiagonal anisotropy has been calculated using the FDTD method.

2. Numerical Stability for Nondiagonal Permittivity Tensor

In the stability analysis, we confirm that the FDTD method for a cloak with a diagonal permittivity tensor cannot directly be extended to the nondiagonal case. Under a coordinate transformation for a cloak [39], material parameters can be expressed as

$$\epsilon^{ij} = \mu^{ij} = \pm\sqrt{g}g^{ij}, \quad (1)$$

where ϵ^{ij} is the relative permittivity, μ^{ij} is the relative permeability, g^{ij} is the metric tensor, and $g = \det g^{ij}$. Because ϵ^{ij} , μ^{ij} are constructed from the symmetric metric tensor g^{ij} , they

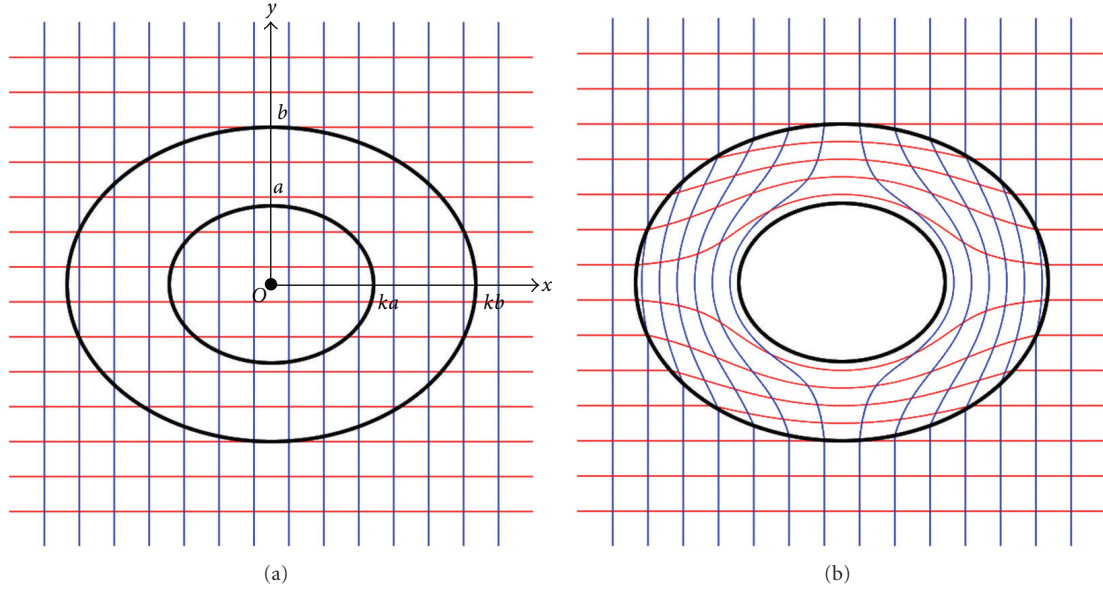


FIGURE 1: Elliptic-cylindrical cloak. (a) Cartesian coordinates: a , b are inner and outer axes; ka , kb are the perpendicular axes. (b) Transformed coordinates.

are symmetric. Consequently, ε^{ij} , μ^{ij} have real eigenvalues with orthogonal eigenvectors and are thus diagonalizable. The eigenvalues, λ , of ε^{ij} , μ^{ij} for an eigenvector \mathbf{V} are defined by

$$\varepsilon^{ij}\mathbf{V} = \mu^{ij}\mathbf{V} = \lambda\mathbf{V}. \quad (2)$$

The phase velocity of light in a material is given by $c = c_0/\lambda$ ($c_0 =$ vacuum light speed), and the Courant-Friedrichs-Lewy (CFL) stability limit becomes

$$\Delta t \leq \frac{\lambda h}{c_0 \sqrt{d}}, \quad (3)$$

where Δt is the time step, h is the grid spacing, and $d = 1, 2,$ and 3 dimensions. Since the FDTD stability depends on the eigenvalues of ε^{ij} and μ^{ij} , to analyze nondiagonal cases, we must first find the eigenvalues and diagonalize ε^{ij} and μ^{ij} . After the diagonalization, the FDTD method for diagonal cases [31–38] can be applied. For diagonal ε^{ij} and μ^{ij} , elements having values less than one are replaced by dispersive quantities to avoid violating the causality and numerical stability [40–44].

In summary, the FDTD modeling for nondiagonal ε^{ij} and μ^{ij} requires three steps:

- (1) find the eigenvalues and eigenvectors and diagonalize the material parameters,
- (2) map the eigenvalues having values less than one to a dispersion model,
- (3) solve Maxwell's equations using the dispersive FDTD method.

3. FDTD Formulation of the Elliptic-Cylindrical Cloak

Two designs of elliptic-cylindrical cloaks have been proposed. One has diagonal ε^{ij} and μ^{ij} in orthonormal elliptic-cylindrical coordinates [45, 46], and in the other ε^{ij} and μ^{ij} are nondiagonal in Cartesian coordinates [47, 48]. We derive a FDTD formulation for the latter in the transverse magnetic (TM) polarization.

3.1. Diagonalization. Figure 1 shows an elliptic-cylindrical cloak in Figure 1(a) Cartesian coordinates and Figure 1(b) transformed coordinates. The inner axis a , the outer axis b , and the perpendicular axes ka and kb are depicted. The elliptic-cylindrical cloak is horizontal when $k > 1$, and vertical when $k < 1$. In the cloak region, $ka \leq \sqrt{x^2 + k^2 y^2} \leq kb$, the material parameters are expressed by

$$\varepsilon^{ij} = \mu^{ij} = \begin{bmatrix} \varepsilon_{xx} & \varepsilon_{xy} & 0 \\ \varepsilon_{xy} & \varepsilon_{yy} & 0 \\ 0 & 0 & \varepsilon_{zz} \end{bmatrix}, \quad (4)$$

where

$$\varepsilon_{xx} = \frac{r}{r-ka} + \frac{k^2 a^2 R^2 - 2kar^3}{(r-ka)r^5} x^2, \quad (5)$$

$$\varepsilon_{xy} = \frac{k^2 a^2 R^2 - ka(1+k^2)r^3}{(r-ka)r^5} xy,$$

$$\varepsilon_{yy} = \frac{r}{r-ka} + \frac{k^2 a^2 R^2 - 2k^3 ar^3}{(r-ka)r^5} y^2, \quad (6)$$

$$\varepsilon_{zz} = \left(\frac{b}{b-a}\right)^2 \frac{r-ka}{r},$$

where $r = \sqrt{x^2 + k^2 y^2}$ and $R = \sqrt{x^2 + k^4 y^2}$. From (4) to (6) we can obtain three eigenvalues

$$\lambda_1 = \frac{\alpha - 1}{\alpha + 1}, \quad \lambda_2 = \frac{1}{\lambda_1}, \quad \lambda_3 = \varepsilon_{zz}, \quad (7)$$

where

$$\alpha = \sqrt{1 + \frac{4r^5(r - ka)}{k^2 a^2 R^2 (x^2 + y^2)}}. \quad (8)$$

Since ε^{ij} is symmetric, it is diagonalized by the eigenvalue matrix Λ and its orthogonal matrix P as follows:

$$\varepsilon^{ij} = P \Lambda P^T, \quad (9)$$

where

$$\Lambda = \begin{bmatrix} \lambda_1 & 0 & 0 \\ 0 & \lambda_2 & 0 \\ 0 & 0 & \lambda_3 \end{bmatrix}, \quad (10)$$

$$P = \begin{bmatrix} \frac{\varepsilon_{xy}}{\beta} & \frac{(\lambda_2 - \varepsilon_{yy})}{\beta} & 0 \\ \frac{(\varepsilon_{yy} - \lambda_2)}{\beta} & \frac{\varepsilon_{xy}}{\beta} & 0 \\ 0 & 0 & 1 \end{bmatrix}, \quad (11)$$

where $\beta = \sqrt{\varepsilon_{xy}^2 + (\lambda_2 - \varepsilon_{yy})^2}$.

3.2. Mapping Eigenvalues to a Dispersion Model. From (7) and (8), λ_1 and λ_3 have values less than one in the cloak region ($ka \leq r \leq kb$). Thus, λ_1 , λ_3 must be replaced by dispersive quantities by using (for example) the Drude model

$$\lambda_i = \varepsilon_{\infty i} - \frac{\omega_{pi}^2}{\omega^2 - j\omega\gamma_i}, \quad (i = 1, 3), \quad (12)$$

where ω is the angular frequency, $\varepsilon_{\infty i}$ is the infinite-frequency permittivity, ω_{pi} is the plasma frequency, and γ_i is the collision frequency. For simplicity, we consider the lossless case, $\gamma_i = 0$. Then the plasma frequencies are given by $\omega_{pi} = \omega\sqrt{\varepsilon_{\infty i} - \lambda_i}$, where $\varepsilon_{\infty i} = \max(1, \lambda_i)$.

3.3. FDTD Discretization. Using the diagonalized material parameters and eigenvalues mapped to the Drude model, we derive an FDTD formulation to solve Maxwell's equations,

$$\begin{aligned} \frac{\partial \mathbf{D}}{\partial t} &= \nabla \times \mathbf{H}, \\ -\frac{\partial \mathbf{B}}{\partial t} &= \nabla \times \mathbf{E}, \end{aligned} \quad (13)$$

where \mathbf{D} is the electric flux density, \mathbf{H} is the magnetic field, \mathbf{B} is the magnetic flux density, and \mathbf{E} is the electric field. In the TM polarization, electromagnetic fields reduce to three nonzero components E_x , E_y , and H_z (D_x , D_y , and B_z). The

D- and **B**-update equations are obtained using Yee algorithm [26–29] as follows:

$$D_x^{n+1} = D_x^n + \frac{\Delta t}{h} d_y H_z^{n+1/2}, \quad (14)$$

$$D_y^{n+1} = D_y^n - \frac{\Delta t}{h} d_x H_z^{n+1/2},$$

$$B_z^{n+3/2} = B_z^{n+1/2} - \frac{\Delta t}{h} (d_x E_y^{n+1} - d_y E_x^{n+1}), \quad (15)$$

where we simply write $D_x(t = n\Delta t) \rightarrow D_x^n$ ($n = \text{integer}$) and d_x, d_y are the spatial difference operators defined by

$$d_x f(x, y) = f\left(x + \frac{h}{2}, y\right) - f\left(x - \frac{h}{2}, y\right), \quad (16)$$

$$d_y f(x, y) = f\left(x, y + \frac{h}{2}\right) - f\left(x, y - \frac{h}{2}\right).$$

To find the **E**-update equations, we consider the relation

$$\mathbf{D} = \varepsilon_0 \varepsilon^{ij} \mathbf{E}, \quad (17)$$

where ε_0 is the vacuum permittivity. From (9), we obtain

$$\varepsilon_0 \mathbf{E} = (\varepsilon^{ij})^{-1} \mathbf{D} = P \Lambda^{-1} P^T \mathbf{D}. \quad (18)$$

Substituting (10) in (18) and multiplying $\lambda_1 \lambda_2$ by both sides, we obtain

$$\varepsilon_0 \lambda_1 \lambda_2 E_x = (\lambda_1 t_2^2 + \lambda_2 t_1^2) D_x + t_1 t_2 (\lambda_1 - \lambda_2) D_y, \quad (19)$$

$$\varepsilon_0 \lambda_1 \lambda_2 E_y = (\lambda_1 t_1^2 + \lambda_2 t_2^2) D_y + t_1 t_2 (\lambda_1 - \lambda_2) D_x, \quad (20)$$

where $t_1 = \varepsilon_{xy}/\beta$ and $t_2 = (\lambda_2 - \varepsilon_{yy})/\beta$. Substituting the Drude model for λ_1 as shown in (12) and using the inverse Fourier transformation rule, $-\omega^2 \rightarrow \partial^2/\partial t^2$, (19) becomes

$$\begin{aligned} \varepsilon_0 \lambda_2 \left(\varepsilon_{\infty 1} \frac{\partial^2}{\partial t^2} + \omega_{p1}^2 \right) E_x &= \left[(\varepsilon_{\infty 1} t_2^2 + \lambda_2 t_1^2) \frac{\partial^2}{\partial t^2} + \omega_{p1}^2 t_2^2 \right] D_x \\ &+ t_1 t_2 \left[(\varepsilon_{\infty 1} - \lambda_2) \frac{\partial^2}{\partial t^2} + \omega_{p1}^2 \right] D_y. \end{aligned} \quad (21)$$

For the discretization, we use the central difference approximation and the central average operator,

$$\begin{aligned} \frac{\partial^2}{\partial t^2} E_x^n &= \frac{E_x^{n+1} - 2E_x^n + E_x^{n-1}}{\Delta t^2}, \\ E_x^n &= \frac{E_x^{n+1} + 2E_x^n + E_x^{n-1}}{4}. \end{aligned} \quad (22)$$

The central average operator improves the stability and accuracy [40, 49, 50]. Similarly, D_x and D_y are discretized, and we obtain the E_x -update equation

$$\begin{aligned} E_x^{n+1} &= -E_x^{n-1} + 2 \frac{a_1^-}{a_1^+} E_x^n + \frac{1}{\varepsilon_0 \lambda_2 a_1^+} \\ &\times \left[b_1^+ (D_x^{n+1} + D_x^{n-1}) - 2b_1^- D_x^n \right. \\ &\left. + c_1^+ (D_y^{n+1} + D_y^{n-1}) - 2c_1^- D_y^n \right], \end{aligned} \quad (23)$$

where D_y^{n+1} , D_y^n , D_y^{n-1} must be spatially interpolated due to the staggered Yee cell [31], and

$$\begin{aligned} a_i^\pm &= \frac{\varepsilon_{\infty i}}{\Delta t^2} \pm \frac{\omega_{pi}^2}{4}, \\ b_i^\pm &= \frac{\varepsilon_{\infty i} t_2^2 + \lambda_2 t_1^2}{\Delta t^2} \pm \frac{\omega_{pi}^2 t_2^2}{4}, \\ c_i^\pm &= t_1 t_2 \frac{\varepsilon_{\infty i} - \lambda_2}{\Delta t^2} \pm \frac{\omega_{pi}^2 t_1^2}{4}. \end{aligned} \quad (24)$$

Similarly, the E_y -update equation is obtained by exchanging $t_1 \leftrightarrow t_2$, $E_x \leftrightarrow E_y$, and $D_x \leftrightarrow D_y$.

To find the H_z -update equation, we consider the relation

$$B_z = \mu_0 \varepsilon_{zz} H_z = \mu_0 \left(\varepsilon_{\infty 3} - \frac{\omega_{p3}^2}{\omega^2} \right) H_z. \quad (25)$$

Analogously to the E_x field, the H_z -update equation can be obtained in the form

$$\begin{aligned} H_z^{n+3/2} &= -H_z^{n-1/2} + 2 \frac{a_3^-}{a_3^+} H_z^{n+1/2} \\ &+ \frac{B_z^{n+3/2} - 2B_z^{n+1/2} + B_z^{n-1/2}}{\mu_0 \Delta t^2 a_3^+}, \end{aligned} \quad (26)$$

where μ_0 is the vacuum permeability.

In summary, the electromagnetic fields are iteratively updated in the following sequence:

- (1) update the components of \mathbf{D}^{n+1} according to (14),
- (2) update the components of \mathbf{E}^{n+1} according to the sample given in (23),
- (3) update the components of $\mathbf{B}^{n+3/2}$ according to (15),
- (4) update the components of $\mathbf{H}^{n+3/2}$ according to (26).

4. Simulation of the Elliptic-Cylindrical Cloak

We calculate electromagnetic propagation for the elliptic-cylindrical cloak using the FDTD formulation shown in Section 3. Figure 2 shows the simulation setup: the computational domain is terminated with a perfectly matched layer in the x -direction, and a periodic boundary condition in the y -direction [29]; the inside of the cloak is covered with a perfect electric conductor (PEC); a plane wave source of wavelength $\lambda_0 = 750$ nm (400 THz) is in the TM polarization; the grid spacing is $h = 10$ nm ($\lambda_0/h = 75$); and the time step is given by the CFL limit, $\Delta t = h/(c_0\sqrt{2})$. Simulation parameters are listed in Table 1.

Figure 3 shows the FDTD results for the elliptic-cylindrical cloak at the steady state (50 wave periods). Figure 3(a) shows calculated H_z field distributions using $h = 10$ nm. The wave propagates without significant disturbance around the cloak, and the calculation is stable. The small ripples on phase planes are purely numerical errors and can be made to vanish by reducing the grid spacing. This can

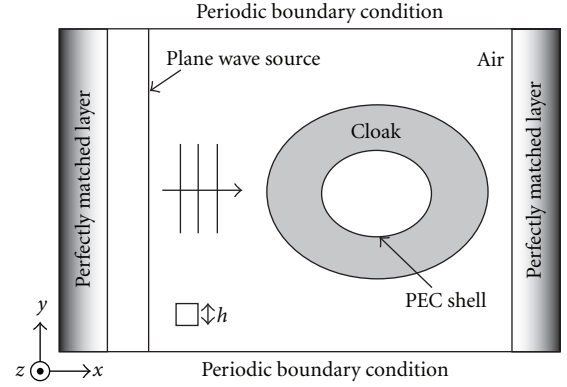


FIGURE 2: Simulation setup of the elliptic-cylindrical cloak for incident TM polarization. Inside of the cloak is covered with a perfect electric conductor (PEC). The gray elliptic region represents the cloak (h : grid spacing).

TABLE 1: Simulation parameters for the elliptic-cylindrical cloak.

Incident wavelength λ_0	750 nm
Inner short semi-axis a	500 nm
Outer short semi-axis b	1000 nm
Axis ratio k	2
Grid spacing h	10 nm
Computational domain	$6 \times 6 \mu\text{m}^2$

be confirmed by calculating the radar cross section (RCS) [29, 51]. In two dimensions, the RCS is defined by

$$\sigma(\phi) = \lim_{r \rightarrow \infty} 2\pi r \frac{|E_s(\phi)|^2}{|E_0|^2}, \quad (27)$$

where ϕ is the scattering angle, $|E_s(\phi)|^2$ is the scattered power in far field, and $|E_0|^2$ is the incident power. If there is no significant disturbance by the object, σ approaches zero. Figure 3(b) shows normalized RCSs on dB scale, σ/λ_0 , scattered by a PEC (without cloak) and cloak using different grid spacings, $h = 20, 10,$ and 5 nm. The PEC or cloak using a coarse grid spacing scatters strongly, but the RCS of the cloak rapidly decreases as the grid spacing is reduced.

Finally, we examine the cloaking performance of the elliptic-cylindrical cloak using the Drude model. Simulation parameters are the same as Table 1 and the cloak is optimized to a wavelength of 750 nm. In the wavelength band, 600 nm–900 nm, we calculate the total cross section (TCS) defined by

$$\sigma_t = \int \sigma(\phi) d\phi. \quad (28)$$

Figure 4(a) shows the calculated TCS spectrum. The TCS rapidly increases with wavelength shifts off the optimal. Figure 4(b) shows the RCS for several wavelengths, A: 730 nm, B: 750 nm, and C: 830 nm (normalized to the RCS for 750 nm). For wavelengths A and C, the scattering is much stronger than the optimal wavelength B.

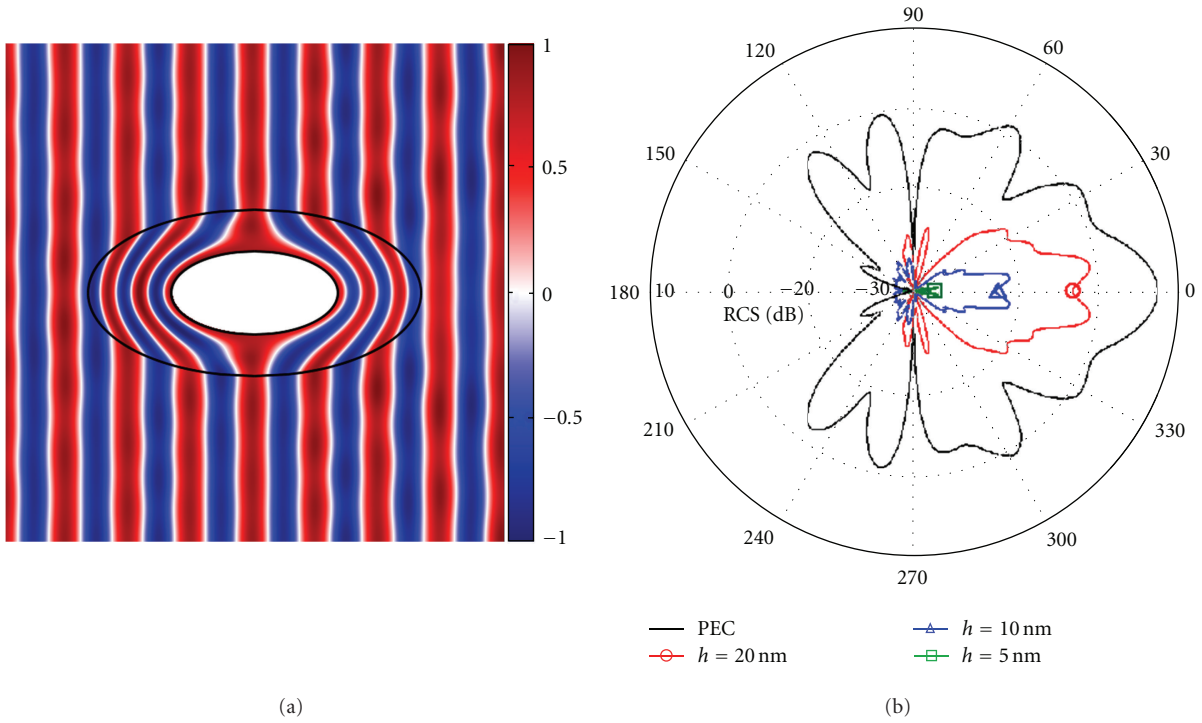


FIGURE 3: FDTD results for the elliptic-cylindrical cloak. (a) H_z field distributions using $h = 10$ nm (black lines are inside and outside shells of the cloak). (b) Radar cross section (RCS) scattered by a PEC (without cloak) and cloak using different grid spacings, $h = 20, 10,$ and 5 nm (radial coordinate is dB).

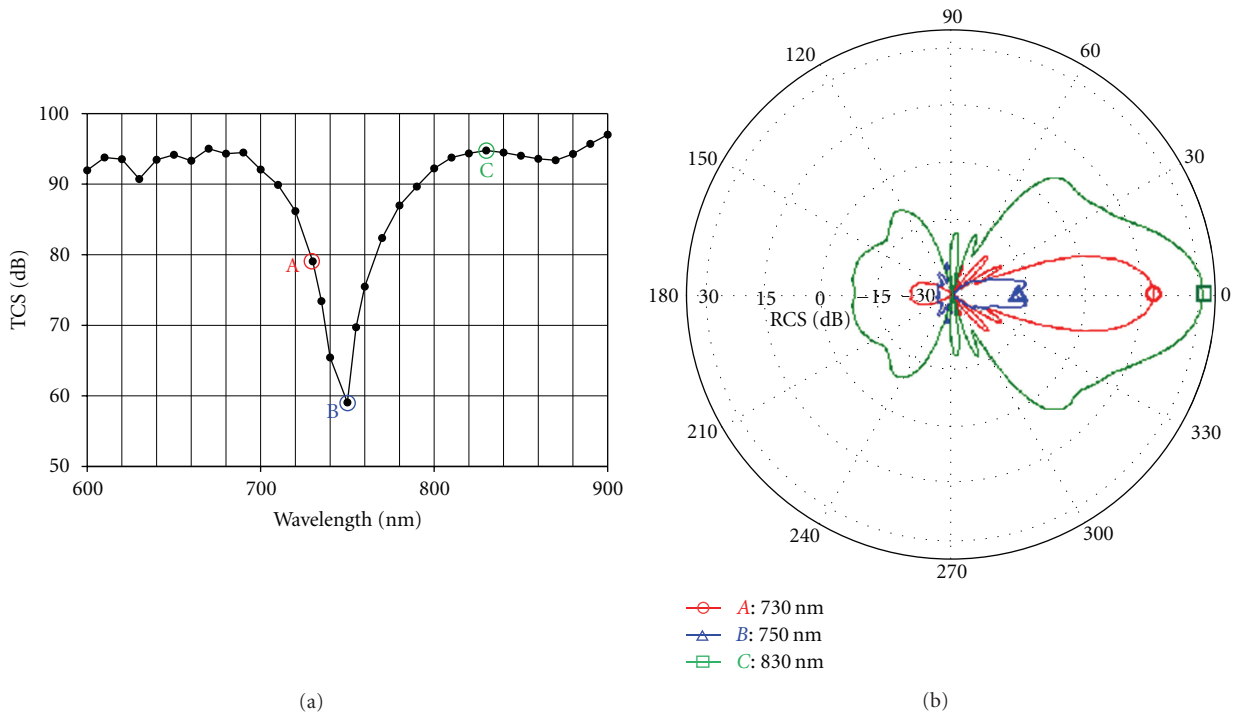


FIGURE 4: Cloaking performance of the elliptic-cylindrical cloak using the Drude model. (a) Total cross section (TCS) spectrum. (b) Sampled RCSs of incident wavelengths, A: 730 nm, B: 750 nm, and C: 830 nm.

5. Conclusion

We describe a stable FDTD modeling procedure for a cloak with a nondiagonal permittivity tensor. When the eigenvalues of the material parameters are less than one, they must be mapped to a dispersion model in order to maintain numerical stability. We implement our method for an elliptic-cylindrical cloak in the TM mode. Numerical calculations demonstrated stable results and the cloaking performance.

Acknowledgment

The authors deeply appreciate the financial support of Grant-in-Aid for Japan Society for the Promotion of Science (JSPS) Fellows.

References

- [1] J. B. Pendry, D. Schurig, and D. R. Smith, "Controlling electromagnetic fields," *Science*, vol. 312, no. 5781, pp. 1780–1782, 2006.
- [2] M. Rahm, D. Schurig, D. A. Roberts, S. A. Cummer, D. R. Smith, and J. B. Pendry, "Design of electromagnetic cloaks and concentrators using form-invariant coordinate transformations of maxwell's equations," *Photonics and Nanostructures Fundamentals and Applications*, vol. 6, no. 1, pp. 87–95, 2007.
- [3] H. Chen and C. T. Chan, "Transformation media that rotate electromagnetic fields," *Applied Physics Letters*, vol. 90, no. 24, Article ID 241105, 2007.
- [4] D. H. Kwon and D. H. Werner, "Polarization splitter and polarization rotator designs based on transformation optics," *Optics Express*, vol. 16, no. 23, pp. 18731–18738, 2008.
- [5] Y. Luo, J. Zhang, B. I. Wu, and H. Chen, "Interaction of an electromagnetic wave with a cone-shaped invisibility cloak and polarization rotator," *Physical Review B*, vol. 78, no. 12, Article ID 125108, 2008.
- [6] T. Zhai, Y. Zhou, J. Zhou, and D. Liu, "Polarization controller based on embedded optical transformation," *Optics Express*, vol. 17, no. 20, pp. 17206–17213, 2009.
- [7] M. Rahm, D. A. Roberts, J. B. Pendry, and D. R. Smith, "Transformation-optical design of adaptive beam bends and beam expanders," *Optics Express*, vol. 16, no. 15, pp. 11555–11567, 2008.
- [8] M. Rahm, S. A. Cummer, D. Schurig, J. B. Pendry, and D. R. Smith, "Optical design of reflectionless complex media by finite embedded coordinate transformations," *Physical Review Letters*, vol. 100, no. 6, Article ID 063903, 2008.
- [9] L. Lan, W. Wei, C. Jianhua, D. Chunlei, and L. Xiangang, "Design of electromagnetic refractor and phase transformer using coordinate transformation theory," *Optics Express*, vol. 16, no. 10, pp. 6815–6821, 2008.
- [10] S. Han, Y. Xiong, D. Genov, Z. Liu, G. Bartal, and X. Zhang, "Ray optics at a deep-subwavelength scale: a transformation optics approach," *Nano Letters*, vol. 8, no. 12, pp. 4243–4247, 2008.
- [11] D. H. Kwon and D. H. Werner, "Transformation optical designs for wave collimators, flat lenses and right-angle bends," *New Journal of Physics*, vol. 10, Article ID 115023, 2008.
- [12] W. X. Jiang, T. J. Cui, G. X. Yu, X. Q. Lin, Q. Cheng, and J. Y. Chin, "Cylindrical-to-plane-wave conver," *Physics Letters*, vol. 92, no. 26, Article ID 261903, 2008.
- [13] Y. Lai, J. Ng, H. Chen et al., "Illusion optics: the optical transformation of an object into another object," *Physical Review Letters*, vol. 102, no. 25, Article ID 253902, 2009.
- [14] W. X. Jiang and T. J. Cui, "Moving targets virtually via composite optical transformation," *Optics Express*, vol. 18, no. 5, pp. 5161–5167, 2010.
- [15] H. Chen, C. T. Chan, and P. Sheng, "Transformation optics and metamaterials," *Nature Materials*, vol. 9, no. 5, pp. 387–396, 2010.
- [16] E. E. Narimanov and A. V. Kildishev, "Optical black hole: broadband omnidirectional light absorber," *Applied Physics Letters*, vol. 95, no. 4, Article ID 041106, 2009.
- [17] D. A. Genov, S. Zhang, and X. Zhang, "Mimicking celestial mechanics in metamaterials," *Nature Physics*, vol. 5, no. 9, pp. 687–692, 2009.
- [18] D. Schurig, J. J. Mock, B. J. Justice et al., "Metamaterial electromagnetic cloak at microwave frequencies," *Science*, vol. 314, no. 5801, pp. 977–980, 2006.
- [19] B. Kanté, D. Germain, and A. De Lustrac, "Experimental demonstration of a nonmagnetic metamaterial cloak at microwave frequencies," *Physical Review B*, vol. 80, no. 20, Article ID 201104, 2009.
- [20] R. Liu, C. Ji, J. J. Mock, J. Y. Chin, T. J. Cui, and D. R. Smith, "Broadband ground-plane cloak," *Science*, vol. 323, no. 5912, pp. 366–369, 2009.
- [21] Y. G. Ma, C. K. Ong, T. Tyc, and U. Leonhardt, "An omnidirectional retroreflector based on the transmutation of dielectric singularities," *Nature Materials*, vol. 8, no. 8, pp. 639–642, 2009.
- [22] H. F. Ma and T. J. Cui, "Three-dimensional broadband ground-plane cloak made of metamaterials," *Nature Communications*, vol. 1, article 21, 2010.
- [23] T. Ergin, N. Stenger, P. Brenner, J. B. Pendry, and M. Wegener, "Three-dimensional invisibility cloak at optical wavelengths," *Science*, vol. 328, no. 5976, pp. 337–339, 2010.
- [24] X. Chen, Y. Luo, J. Zhang, K. Jiang, J. B. Pendry, and S. Zhang, "Macroscopic invisibility cloaking of visible light," *Nature Communications*, vol. 2, article 176, 2011.
- [25] J. Zhang, L. Liu, Y. Luo, S. Zhang, and N. A. Mortensen, "Homogeneous optical cloak constructed with uniform layered structures," *Optics Express*, vol. 19, no. 9, pp. 8625–8631, 2011.
- [26] K. Yee, "Numerical solution of initial boundary value problems involving maxwell's equations in isotropic media," *IEEE Transactions on Antennas and Propagation*, vol. 14, no. 3, pp. 302–307, 1966.
- [27] A. Taflove and M. E. Brodwin, "Numerical solution of steady-state electromagnetic scattering problems using the time-dependent maxwell's equations," *IEEE Transactions on Microwave Theory and Techniques*, vol. 23, no. 8, pp. 623–630, 1975.
- [28] A. Taflove, "Application of the finite-difference time-domain method to sinusoidal steady-state electromagnetic-penetration problems," *IEEE Transactions on Electromagnetic Compatibility*, vol. 22, no. 3, pp. 191–202, 1980.
- [29] A. Taflove and S. C. Hagness, *Computational Electrodynamics: The Finite-Difference Time-Domain Method*, Artech House, Norwood, Mass, USA, 3rd edition, 2005.
- [30] E. Kallos, C. Argyropoulos, and Y. Hao, "Ground-plane quasicloaking for free space," *Physical Review A*, vol. 79, no. 6, Article ID 063825, 2009.
- [31] Y. Zhao, C. Argyropoulos, and Y. Hao, "Full-wave finite-difference time-domain simulation of electromagnetic cloaking structures," *Optics Express*, vol. 16, no. 9, pp. 6717–6730, 2008.

- [32] Y. Hao and R. Mittra, *FDTD Modeling of Metamaterials: Theory and Applications*, Artech House, Norwood, Mass, USA, 1st edition, 2008.
- [33] J. A. Silva-Macêdo, M. A. Romero, and B. H. V. Borges, "An extended FDTD method for the analysis of electromagnetic field rotations and cloaking devices," *Progress in Electromagnetics Research*, vol. 87, pp. 183–196, 2008.
- [34] C. Argyropoulos, Y. Zhao, and Y. Hao, "A radially-dependent dispersive finite-difference time-domain method for the evaluation of electromagnetic cloaks," *IEEE Transactions on Antennas and Propagation*, vol. 57, no. 5, pp. 1432–1441, 2009.
- [35] C. Argyropoulos, E. Kallos, Y. Zhao, and Y. Hao, "Manipulating the loss in electromagnetic cloaks for perfect wave absorption," *Optics Express*, vol. 17, no. 10, pp. 8467–8475, 2009.
- [36] C. Argyropoulos, E. Kallos, and Y. Hao, "Dispersive cylindrical cloaks under nonmonochromatic illumination," *Physical Review E*, vol. 81, no. 1, Article ID 016611, 2010.
- [37] C. Argyropoulos, E. Kallos, and Y. Hao, "FDTD analysis of the optical black hole," *Journal of the Optical Society of America B*, vol. 27, no. 10, pp. 2020–2025, 2010.
- [38] C. Argyropoulos, E. Kallos, and Y. Hao, "Bandwidth evaluation of dispersive transformation electromagnetics based devices," *Applied Physics A*, vol. 103, no. 3, pp. 715–719, 2011.
- [39] U. Leonhardt and T. G. Philbin, "Chapter 2 transformation optics and the geometry of light," *Progress in Optics*, vol. 53, pp. 69–152, 2009.
- [40] J. A. Pereda, L. A. Vielva, A. Vegas, and A. Prieto, "Analyzing the stability of the FDTD technique by combining the von neumann method with the Routh-Hurwitz criterion," *IEEE Transactions on Microwave Theory and Techniques*, vol. 49, no. 2, pp. 377–381, 2001.
- [41] G. V. Eleftheriades and K. G. Balmain, *Negative Refraction Metamaterials: Fundamental Principles and Applications*, Wiley-IEEE Press, New York, NY, USA, 1st edition, 2005.
- [42] S. A. Tretyakov and S. I. Maslovski, "Veselago materials: what is possible and impossible about the dispersion of the constitutive parameters," *IEEE Antennas and Propagation Magazine*, vol. 49, no. 1, pp. 37–43, 2007.
- [43] P. Yao, Z. Liang, and X. Jiang, "Limitation of the electromagnetic cloak with dispersive material," *Applied Physics Letters*, vol. 92, no. 3, Article ID 031111, 2008.
- [44] Z. Lin and L. Thylén, "On the accuracy and stability of several widely used FDTD approaches for modeling lorentz dielectrics," *IEEE Transactions on Antennas and Propagation*, vol. 57, no. 10, pp. 3378–3381, 2009.
- [45] H. Ma, S. Qu, Z. Xu, J. Zhang, B. Chen, and J. Wang, "Material parameter equation for elliptical cylindrical cloaks," *Physical Review A*, vol. 77, no. 1, Article ID 013825, 2008.
- [46] E. Cojocaru, "Exact analytical approaches for elliptic cylindrical invisibility cloaks," *Journal of the Optical Society of America B*, vol. 26, no. 5, pp. 1119–1128, 2009.
- [47] W. X. Jiang, T. J. Cui, G. X. Yu, X. Q. Lin, Q. Cheng, and J. Y. Chin, "Arbitrarily elliptical-cylindrical invisible cloaking," *Journal of Physics D*, vol. 41, no. 8, Article ID 085504, 2008.
- [48] T. J. Cui, D. R. Smith, and R. Liu, *Metamaterials: Theory, Design, and Applications*, Springer, New York, NY, USA, 1st edition, 2009.
- [49] F. B. Hildebrand, *Introduction to Numerical Analysis*, Dover Publications, New York, NY, USA, 2nd edition, 1987.
- [50] Y. Zhao, P. A. Belov, and Y. Hao, "Modelling of wave propagation in wire media using spatially dispersive finite-difference time-domain method: numerical aspects," *IEEE Transactions on Antennas and Propagation I*, vol. 55, no. 6, pp. 1506–1513, 2007.
- [51] K. S. Kunz and R. J. Luebbers, *The Finite Difference Time Domain Method for Electromagnetics*, CRC Press, New York, NY, USA, 1st edition, 1993.



Hindawi

Submit your manuscripts at
<http://www.hindawi.com>

